The Simulation of the Preparation of the Ingot With Liquid Core

yongqiang wu
University of Science and Technology Beijing
Zhi-ren Sun
School of Materials Science and Engineering, University of Science and Technology Beijing, Beijing 100083, China
Kaikun Wang (kkwang@mater.ustb.edu.cn)
School of Materials Science and Engineering, University of Science and Technology Beijing, Beijing 100083, China

Research Article

Keywords: solidification, the ultra-high temperature demoulding, the equivalent coefficient, the boundary conditions, DEFORM-3D, the method of solidification time, DEFORM-2D

Posted Date: March 26th, 2021

DOI: https://doi.org/10.21203/rs.3.rs-346503/v1

Abstract

During the preparation of the ingot with liquid core in the early stage, the finite element models of the solidification and the ultra-high temperature demoulding were established in DEFORM-3D. The thermophysical properties of ASSAB 718 with the variations of C, Mn and Cr were calculated in JMatPro®. The material database was imported into DEFORM-3D. Through the analysis of the finite element simulation results, we obtained the influence of three main elements C, Mn and Cr contents on the size of the solid-phase region, the liquid-phase region and the solid-liquid two-phase region in the ingot. We optimized the composition of the material to get a wide solid-liquid phase range. The high carbon, the medium manganese and the high chromium contents were beneficial to form the liquid core. Based on the method of the solidification time, the algorithm was programmed by the python language. We analyzed the influence of the three elements C, Mn, and Cr on the concentration distribution based on the temperature field data, which were obtained by DEFORM-2D after the solidification and the ultra-high temperature demoulding. According to the simulation results, we found that the region prone to negative segregation.

1 Introduction

In recent years, the rapid developments of the world industry significantly increase large forgings requirements, such as shipbuilding, electric power, petroleum, etc. Quality requirements also become higher and higher. With the development of major equipment to high-performance, large-scale, integrated and safer direction, forging process innovation has attracted the industry's attention. Compared with traditional forging, a green and short-flow forging process[1–3] has been proposed and implemented since 2014. That is the liquid core forging process. The cast ingot is demoulded with liquid core at ultra-high temperature and then forged with liquid core at high temperature. It is a forming method between casting and forging. The liquid core is under pressure and the dendrites are broken to form a uniform and fine structure. It also makes the performance of the material more uniform after forging. So the preparation processes of the ingot with liquid core are worth studying. Those processes include the solidification with mold and the ultra-high temperature demoulding. As a short-flow process, we need to understand the influence of the material compositions on the liquid region and the distribution of the elements during the preparation of the ingot with liquid core.

Dong Jie et al.[4–5] used the commercial finite element analysis software ANSYS for the three-dimensional temperature field and the ingot mold's thermal stress field during the solidification process. But the research only took into the conventional solidification process. Zhao Xuezhi et al. [6] simulated the heating process with software DEFORM-3D and the process parameters were optimized adapting orthogonal test. The temperature field and the stress field during heating were analyzed. Zong Weiqi et al. [7] used the DEFORM-3D software to simulate the heating process of the ingot during high temperature charging. The distribution of the temperature field and the stress field of the ingot during heating were obtained. The results showed that the high temperature charging could effectively reduce the heating

time. The above two processes use the DEFORM-3D to study the heating process of the ingot but do not study the solidification process.

The DEFORM software [8] simulates the two preparation processes including the solidification and the ultra-high temperature demoulding during the preparation of the ingot with liquid core. The software has a user-defined material database which allows users to input materials that are not in the material database. For heat conduction analysis, the equilibrium equations, constitutive relations, and boundary conditions are first converted into nonlinear equations through a finite element discretization. Then they will be solved by the direct iteration method and the Newton-Raphson method. The user can obtain the required results in the post-processor. The contours of the temperature field variables are drawn to make the post-processing simple and straightforward. We studied the influence of three main elements C, Mn and Cr contents on the size of the liquid core during the preparation of the ingot with liquid core by DEFORM-3D. We also studied the distribution of those elements by DEFORM-2D. According to the temperature field distribution, the solid-phase region, the liquid-phase region and the solid-liquid two-phase region can be distinguished. By using the temperature data from DEFORM-2D, the nodal concentration of the ingot was calculated. The distribution of C, Mn, Cr three elements were obtained which provided a theoretical basis for the preparation process of the ingot with liquid core.

2 Model Establishment

2.1 Assumptions of the simulation conditions

To ensure the regular operation of the software and the accuracy of the simulation, we made the following simplifications and hypothesis:

(1) In the geometric model, only the solidification of the ingot body was considered. According to the literature, the thermal influence of the ingot mold, the insulation board and the base plate were converted into the equivalent heat transfer coefficient[9–10], which would be loaded on the corresponding boundary conditions.

(2) It was only considered that the solidification occurred when the ingot temperature was cooled below the liquidus temperature.

(3) The initial simulation conditions of the ingot were the same. In DEFORM-3D, each region's volume was replaced by the number of unit nodes located in the solid-phase region, the liquid-phase region and the solid-liquid two-phase region. In DEFORM-2D, the unit area replaced the volume of each region.

These simplifications and hypotheses were beneficial to the analysis of the solidification and the ultra-high temperature demoulding. The internal temperature field of the liquid core ingot could be simulated more accurately.

2.2 Establishment of the finite element model

The material used in the finite element model is ASSAB 718[11–12]. The steel grade is usually supplied in the prehardened condition and can be placed in service directly after machining. It can be used to make large and high-grade plastic mold parts. The composition is shown in Table 1, which refers to the weight percent. The initial casting temperature is 1530℃ and the pre-heated temperature of the mold is 80°C. Through the calculation of JMatPro®, the liquidus temperature of ASSAB 718 is 1487℃ and the solidus temperature is 1423℃. JMatPro®[13–15] is a powerful material performance simulation software and can be used to calculate various metal materials' properties. We also obtained the thermophysical properties of ASSAB 718 from the software, as shown in Fig. 1. The calculated material properties were built into the database and then imported into the DEFORM-3D software.

Table 1
Chemical compositions of ASSAB 718 (wt.%)

Material	C	Si	Mn	P	S	Cr	Mo	Ni
Wt/%	0.34–0.40	0.20–0.40	1.20–1.60	≤ 0.015	≤ 0.010	1.70–2.10	0.27–0.37	0.95–1.15

The ingot is octagonal and the specific sizes are shown in Table 2 with 10017 nodes and 47017 grid elements. The height to diameter ratio and the preliminary ingot taper are 1.5 and 3.93%, respectively[16], which are proper according to the widely accepted censuses.

Table 2
Ingot parameters

Ingot type	Riser height (mm)	Ingot body height (mm)	Length of large head side(mm)	Length of small head side(mm)
Regular octagonal plum blossom ingot	300	1400	1025	915

The casting material is gray cast iron, which contains 3.3–3.9%C, 0.6–0.9%Mn, 1.8–2.3%Si, P < 0.15 and S < 0.12. The wall thickness of the ingot mold is 175 mm[17]. The thermal conductivity of this material is shown in Table 3.

Table 3
The thermal conductivity of the ingot mold

Temperature/℃	Thermal conductivity/cal/(cm·s·℃)
20	0.186
200	0.141
400	0.104
800	0.07
1200	0.036

3 Influences of C, Mn, Cr element contents on three regions

3.1 Different carbon contents

Table 4 showed the chemical compositions of ASSAB 718 when the carbon weight percents were 0.34%, 0.37%, 0.4% and the thermophysical properties were calculated by JMatPro® software.

Table 4
Chemical compositions of ASSAB 718 with different carbon contents (wt.%)

C	Si	Mn	P	S	Cr	Mo	Ni
0.34	0.3	1.4	0.01	0.008	1.9	0.33	1
0.37	0.3	1.4	0.01	0.008	1.9	0.33	1
0.40	0.3	1.4	0.01	0.008	1.9	0.33	1

The solidification rates of the ingot were different: the bottom solidified first and the riser solidified last. The solidification followed the sequence: moving from the bottom to the top in the axial direction and extending from the surface to the center in the radial direction. At the beginning of the solidification, there was an appreciably longitudinal temperature gradient in the lower part of the ingot. With time, the cooling effect from the bottom became smaller and the cooling effect was reduced. So the longitudinal temperature gradient gradually decreased. In the middle part of the ingot, the liquid phase remained unchanged at first. Then the longitudinal temperature gradient increased with the decrease of the temperature, but the change was not noticeable. We got the ingot's temperature field after the solidification process with mold in the simulation of DEFORM-3D software. From 10017 nodes' temperature data, we got the numbers of the nodes which were located in the liquid-phase region, the solid-liquid two-phase region and the solid-phase region. When the carbon content was 0.34%, there were 2104 nodes in the liquid-phase region, accounting for 21.49% of the total number. Those were about 9% lower than those with 0.37% and 0.4% carbon contents as shown in Fig. 3. The nodes in the solid-liquid two-phase region were about 9% more than those of 0.37% and 0.4% carbon contents and the ones in the solid-phase region were almost the same under the three components.

We got the temperature field distribution of the ingot after the ultra-high temperature demoulding in the simulation of DEFORM-3D software. When the carbon content was 0.34%, the nodes in the liquid-phase region decreased to 2.7%. The ones in the solid-liquid two-phase region were about 5% lower than those of 0.37% and 0.4% carbon contents. The nodes in the solid-phase region were about 6% higher, as shown in Fig. 4.

Under the same conditions, the medium and high carbon contents of ASSAB 718 were beneficial to forming the liquid core.

3.2 Different manganese contents

Table 5 showed the chemical compositions of ASSAB 718 when the manganese weight percents were 1.2%, 1.4%, 1.6%. The thermophysical properties were calculated by JMatPro® software.

Table 5
Chemical compositions of ASSAB 718 with different manganese contents (wt.%).

C	Si	Mn	P	S	Cr	Mo	Ni
0.37	0.3	1.2	0.01	0.008	1.9	0.33	1
0.37	0.3	1.4	0.01	0.008	1.9	0.33	1
0.37	0.3	1.6	0.01	0.008	1.9	0.33	1

We got the ingot's temperature field during the solidification process with mold in the simulation of DEFORM-3D software. From 10017 nodes' temperature data, we obtained the numbers of the nodes which were located in the liquid-phase region, the solid-liquid two-phase region and the solid-phase region. When the manganese content was 1.4%, there were 3106 nodes in the liquid-phase region, accounting for 30.92% of the total number. They were about 9% higher than those with 1.2% and 1.6% manganese contents, as shown in Fig. 5. The nodes in the solid-liquid two-phase region were about 9% less than those of 1.2% and 1.6% manganese contents. The nodes in the solid-phase region were almost the same under the three components.

We got the temperature field distribution of the ingot after the ultra-high temperature demoulding in the simulation of DEFORM-3D software. When the manganese content was 1.4%, the nodes in the liquid-phase region decreased to 4.43%. The nodes in the solid-liquid two-phase region were about 5% higher than those of 1.2% and 1.6% of manganese contents. The nodes in the solid-phase region were about 6% lower, as shown in Fig. 6.

Under the same conditions, the medium manganese content of Assab 718 was beneficial to forming the liquid core.

3.3 Different chromium contents

Table 6 showed the chemical compositions of ASSAB 718 when the chromium weight percents were 1.7%, 1.9%, and 2.1%. The thermophysical properties were calculated by JMatPro® software.

Table 6
Chemical compositions of ASSAB 718 with different chromium contents (wt.%)

C	Si	Mn	P	S	Cr	Mo	Ni
0.37	0.3	1.4	0.01	0.008	1.7	0.33	1
0.37	0.3	1.4	0.01	0.008	1.9	0.33	1
0.37	0.3	1.4	0.01	0.008	2.1	0.33	1

We got the temperature field of the ingot after the solidification process with mold in the simulation of DEFORM-3D software. From 10017 nodes' temperature data, we obtained the numbers of the nodes which were located in the liquid-phase region, the solid-liquid two-phase region and the solid-phase region. When the chromium content was 1.7%, there were 2204 nodes in the liquid-phase region, accounting for 21.58% of the total number, which was about 10% lower than those with 1.9% and 2.1% chromium contents as shown in Fig. 7. The nodes in the solid-liquid two-phase region were about 9% more than those of 1.9% and 2.1% chromium contents and the ones in the solid-phase region were almost the same under the three components.

We got the temperature field distribution of the ingot after the ultra-high temperature demoulding in the simulation of DEFORM-3D software. When the chromium content was 1.7%, the nodes in the liquid region decreased to 2.88%. The ones in the solid-liquid two-phase region were about 5% lower than those of 1.9% chromium content while they were about 7% lower than those of 2.1% chromium content. The nodes in the solid-phase region were about 6% higher than those of 1.9% chromium content while they were about 8% higher than those of 2.1% chromium content, as shown in Fig. 8.

Under the same conditions, the high chromium content of Assab 718 was beneficial to forming the liquid core.

Through the analysis of finite element simulation results, we obtained the influence of three main elements C, Mn and Cr contents on the size of the solid-phase region, the liquid-phase region and the solid-liquid two-phase region in the ingot. We optimized the composition of the material to get a wide solid-liquid phase range. The high carbon, the medium manganese and the high chromium contents were beneficial to forming the liquid core.

4 Influences On Temperature Differences

The ingot's initial temperature and the temperature after solidification with mold were obtained from the temperature field in DEFORM-3D. We calculated the temperature difference of each node. The maximum temperature differences, the minimum temperature differences and the average temperature differences

were shown in Fig. 9(a-c) with the change of C, Mn and Cr contents. We also calculated the temperature differences of 10017 nodes before and after the ultra-high temperature demoulding. The maximum temperature differences, the minimum temperature differences and the average temperature differences were shown in Fig. 9(d-e) with the change of C, Mn and Cr contents. It was seen that the changes in the contents of C, Mn, and Cr did not affect the temperature differences. During the solidification process with mold, the maximum temperature differences was 660 ± 5°C, the minimum temperature differences was 10 ± 5°C, and the average temperature differences was 220 ± 10°C. After the ultra-high temperature demoulding, the maximum temperature differences was 260 ± 5°C, the minimum temperature differences was 10 ± 5°C, and the average temperature differences was 50 ± 10℃.

From the above results, it can be obtained that the change of chemical elements only affect the size of the solid-phase region, the liquid-phase region and the solid-liquid two-phase region, but has no significant effect on the solidification rate.

5 The Simulation Of The Elements Distribution

5.1 Theoretical basis

The method of solidification time[18–19] is the time that it takes for a unit in the ingot to drop from the liquidus temperature to the solidus temperature. The method of solidification time refers to the residence time of molten steel in the solid-liquid two-phase region. The region with longer solidification time also takes longer to enrich solute, so the macro-segregation possibility is more significant. The method of solidification time is determined by the temperature changes in each region of the ingot. Therefore, we calculate the concentration according to the temperature history during the solidification process. The macro-segregation occurs on the contour surface with the different concentrations.

5.2 Calculation method of the concentration

For the solidification process of the large ingots, the total mass of solute enriched from the solid-liquid two-phase region to the liquid-phase region at the current moment was expressed as the concentration variation $\triangle C$ multiplied by the total volume V_{LS} of the solid-liquid two-phase region. Therefore, the increase of liquid concentration was equal to the total mass of solute enriched in the solid-liquid two-phase region $\triangle C \times V_{LS}$ divided by the total volume V_L in the liquid-phase region. So we got the following formula[18–19]:

(1) If the region were located in the solid-liquid two-phase region, the concentration would change to $C-\triangle C$ based on the original concentration C;

(2) If the region were located in the liquid-phase region, the concentration would change to $C+\triangle C \times V_{LS} / V_L$ based on the original concentration C;

(3) The concentration of all the regions in the solid-phase did not change.

C and △C are the volumetric concentration with the unit t/m^3. The concentration variation △C is mainly affected by the element type and the solidification time. Based on the python language, the nodal concentration of the ingot was calculated by using the temperature data simulated by DEFORM-2D.

5.3 Model establishment

ASSAB 718 is often used after heat treatment (hardened and tempered), which solves the problems of macro-segregation. The new approach we adopt to reduce the segregation is before the heat treatment. ASSAB 718 used in the model has 0.37%C, 1.4%Mn and 1.9%Cr. The effects on the distribution of C, Mn, and Cr were studied during the preparation of the ingots with liquid core[20]. The ingot's longitudinal section in the center was selected as the research object by the section method. Half of the longitudinal section was simulated in the DEFORM-2D software. The two-dimensional model had the same temperature field as the longitudinal section of the three-dimensional model, as shown in Fig. 10.

Due to the advantages of the DEFORM software in calculating the temperature field and exporting data, we got the nodes' temperatures after the solidification with mold and after the ultra-high temperature demoulding. We wrote the program in the python language based on the simulation of the temperature field. And we used the method of solidification time to get the distribution of the elements in the ingot with liquid core.

5.4 The simulation results

Figure 11 (a) showed the concentration distributions of C after the solidification with mold and Fig. 11 (b) showed the concentration distributions after the ultra-high temperature demoulding[21–22]. The highest concentration was in front of the solidification and the lowest occurred within 500–700 mm from the ingot's bottom. Figure 11 (c-d) showed Mn's concentration distributions after the solidification with mold and the ultra-high temperature demoulding separately. Figure 11 (e-f) showed Cr's concentration distributions after the solidification with mold and the ultra-high temperature demoulding separately. As could be seen from the figures, Mn and Cr showed the same distributions as C. The highest concentration was in front of the solidification and the lowest occurred within 500–700 mm from the ingot's bottom. A negative segregation zone was easy to form at the lowest concentration and the element content increased more gently from the surface to the center. Compared with the traditional process, the ultra-high temperature demoulding process of the ingot is a drastically change process. The new technology shortens the diffusion time and the solidification time of three main elements C, Mn and Cr. 500–700 mm from the ingot's bottom is in the solid-liquid two-phase region for a longer time, so it is prone to negative segregation.

According to the simulation results, we developed a subsequent forging process with liquid core to reduce the macro-segregation. Under the external pressure, the solute diffusion velocity was changed. The element segregation was reduced and the forging with uniform composition was obtained.

5.5 Comparison of simulation models

In order to ensure the accuracy of the simulation, the thermal boundary conditions used in the simulation were obtained from the actual production data. We also made a comparison with G. Lesoult's research. G. Lesoult showed us the segregation in the 65t steel ingot in the paper "Macrosegregation in steel strands and ingots: Characterization, formation and consequences". The carbon content at the bottom of the ingot was less than the nominal one. It occupies more than 50% of the height in the center of the ingot, like the globular equiaxed zone[22].

6 Conclusion

According to the data obtained by the finite element software DEFORM, we get the influences of C, Mn, Cr three elements on the solid-phase region, the liquid-phase region and the solid-liquid two-phase region in the preparation of the ingot with liquid core. We also analyzed the distribution of C, Mn, Cr three elements after the solidification process with mold and the ultra-high temperature demoulding. The following conclusions are drawn:

1. During the ingot preparation with liquid core, the liquid-phase region is the largest with the high carbon, the medium manganese and the high chromium. It provides suitable conditions for the formation of liquid core in the forging process;

2. Based on the method of solidification time, the concentration distribution is calculated. A negative segregation zone is easy to form within 500–700 mm from the ingot's bottom.

Declarations

Ethical Approval and Consent to Participate

Not applicable.

-Consent to Publish

- that the work described has not been published before (except in the form of an abstract or as part of a published lecture, review, or thesis).
- that it is not under consideration for publication elsewhere;
- that its publication has been approved by all co-authors, if any;
- that its publication has been approved (tacitly or explicitly) by the responsible authorities at the institution where the work is carried out.

-Authors Contributions

Kaikun Wang contributed to the conception of the study;

Yongqiang Wu performed the experiment, contributed significantly to analysis and manuscript preparation, performed the data analyses and wrote the manuscript;

Sun Zhi-ren used the python language to program the solidification time method.

-Funding

This work was financially supported by the National Key Research and Development Program of China (2017YFB0701803&2017YFB0701801).

-Competing Interests

The authors declare that they have no known competing financial interests or personal relationships that could have appeared to influence the work reported in this paper.

-Availability of data and materials

The data used to support the findings of this study are included within the article.

Acknowledgements

The authors would like to sincerely thank the National Key Research and Development Program of China (2017YFB0701803&2017YFB0701801 for the financial support.

References

[1] Wang KK (2015) The current situation and thinking of material processing industry in Gansu Province. Love Longyuan. In: The 15th batch of achievements of Doctor Service Group on probation:221–223.

[2] Wang KK, Fu W, Hu ZQ (2017) A high uniformity short process forming method for large metal components [P].China: ZL201711262274.8

[3] Wu YQ, Wang KK, Ruan SR (2021) A new forging technology of 19 tons flat ingot with semi-solid liquid core[J]. The International Journal of Advanced Manufacturing Technology, Vol.112(9-10):2899-2908. https://doi.org/10.1007/s00170-020-06524-y

[4]Dong J(2005) Numerical Simulation of Temperature and Thermal Stress Fieldin Steel Ingot Solidification Process and Application[D]. Xi'an University of Architecture and Technology, Xi'an.

[5] Dong J, Yuan SQ, Deng LT, Liu XY (2007) Numerical Simulation of Temperature Field in Steel Ingot Solidification Process[J]. Foundry Technology. Vol.28: 268-270.

[6] Zhao XZ, Fan YB, Xia QX, Lu MK, Du YL (2013) Research and Optimization of Heating Process Before Forging for 5CrNiMo Hot Working Die Steel[J]. Hot Working Technology. Vol.42:110-113.

[7] Zong WQ, Wu Z, Shan HX, Xia QX(2012) Distributions of Temperature and Stress During Ingot Heating when Charging at High Temperature[J]. Hot Working Technology. Vol.41: 4-7.

[8] Scientific Forming Technologies Corporation. DEFORM 3D^{TM} Version 6.0 User's Manual, Part 1: 10-16.

[9] P. Martins J, Neto D, Alves J, Oliveira M, Menezes L (2016) Numerical modeling of the thermal contact in metal forming processes[J]. The International Journal of Advanced Manufacturing Technology, Vol.87(5):1797-1811. https://doi.org/10.1007/s00170-016-8571-y

[10] Cebo, A (2010)The effect of the error of thermal conductivity, specific heat and density determination on the inverse calculation of the heat transfer coefficient[J]. Archives of metallurgy and materials, Vol.55(2):429-434.

[11] Tlhabadira I, Daniyan I, Machaka R, Machio C, Masu L, VanStaden L(2019) Modelling and optimization of surface roughness during AISI P20 milling process using Taguchi method[J]. The International Journal of Advanced Manufacturing Technology, Vol.102(9):3707-3718. https://doi.org/10.1007/s00170-019-03452-4

[12] He YL, Gao W, Li L, Wang QL, Ye P(2004) Effect of Heat Treatment on Machinability of 718 Plastic Die Steel[J]. Heat Treatment of Metals, Vol, 29: 20-23. (in Chinese)

[13] Olovsjö S, Hammersberg P, Avdovic P, Ståhl J, Nyborg L(2012) Methodology for evaluating effects of material characteristics on machinability—theory and statistics-based modelling applied on Alloy 718[J]. The International Journal of Advanced Manufacturing Technology, Vol.59(1):55-66. https://doi.org/10.1007/s00170-011-3503-3

[14] Saunders N, Guo U, Li X, Miodownik A, Schillé J(2003) Using JMatPro to model materials properties and behavior[J]. JOM, Vol.55: 60-65. https://doi.org/10.1007/s11837-003-0013-2

[15] Schillé, Jean-P, Guo ZL, Saunders N, Miodownik, A. Peter(2011)Modeling Phase Transformations and Material Properties Critical to Processing Simulation of Steels[J]. Materials and Manufacturing Processes, Vol.26: 137-143. https://doi.org/10.1080/10426910903153059

[16] Vasko F, Wolf F, Stott K, Scheirer J(1989)Selecting Optimal Ingot Sizes for Bethlehem Steel. Interfaces, Vol.19(1):68-84. https://doi.org/10.1287/inte.19.1.68

[17] Kermanpur A, Eskandari M, Purmohamad H, Soltani MA, Shateri R (2010) Influence of mould design on the solidification of heavy forging ingots of low alloy steels by numerical simulation[J]. Materials in engineering, Vol.31(3): 1096-1104.

https://doi.org/10.1016/j.matdes.2009.09.045

[18] Ren HJ, Liang XP (2012) Prediction of Macro Segregation to Heavy Ingots by Advanced Solidification Time Method[J]. Heavy Casting and Forging,Vol.1: 1-5. (in Chinese)

[19] Ren HJ(2011) The Algorithm Research to the Macro Segregation Prediction of the Heavy Ingot Solidification Process[D]. Chongqing University, Chongqing. (in Chinese)

[20] Haida O, Okano S, Emi T, Kasai G(1981) Estimating the Formation of A-Segregation in a Steel Ingot in Terms of the Chemical Composition of the Steel[J]. Tetsu-to-Hagane, 67□7□: 954~958.

[21] Schneider MC, Beckermann C(1995) Simulation of Micro-/macrosegregation during the Solidification of a Low-Alloy Steel[J]. Isij International, Vol.35(6): 665-672.

[22] Lesoult, G(2005) Macrosegregation in steel strands and ingots: Characterization, formation and consequences[J]. Materials science & engineering. A, Structural materials, Vol.413:19-29. https://doi.org/10.1016/j.msea.2005.08.203

Figures

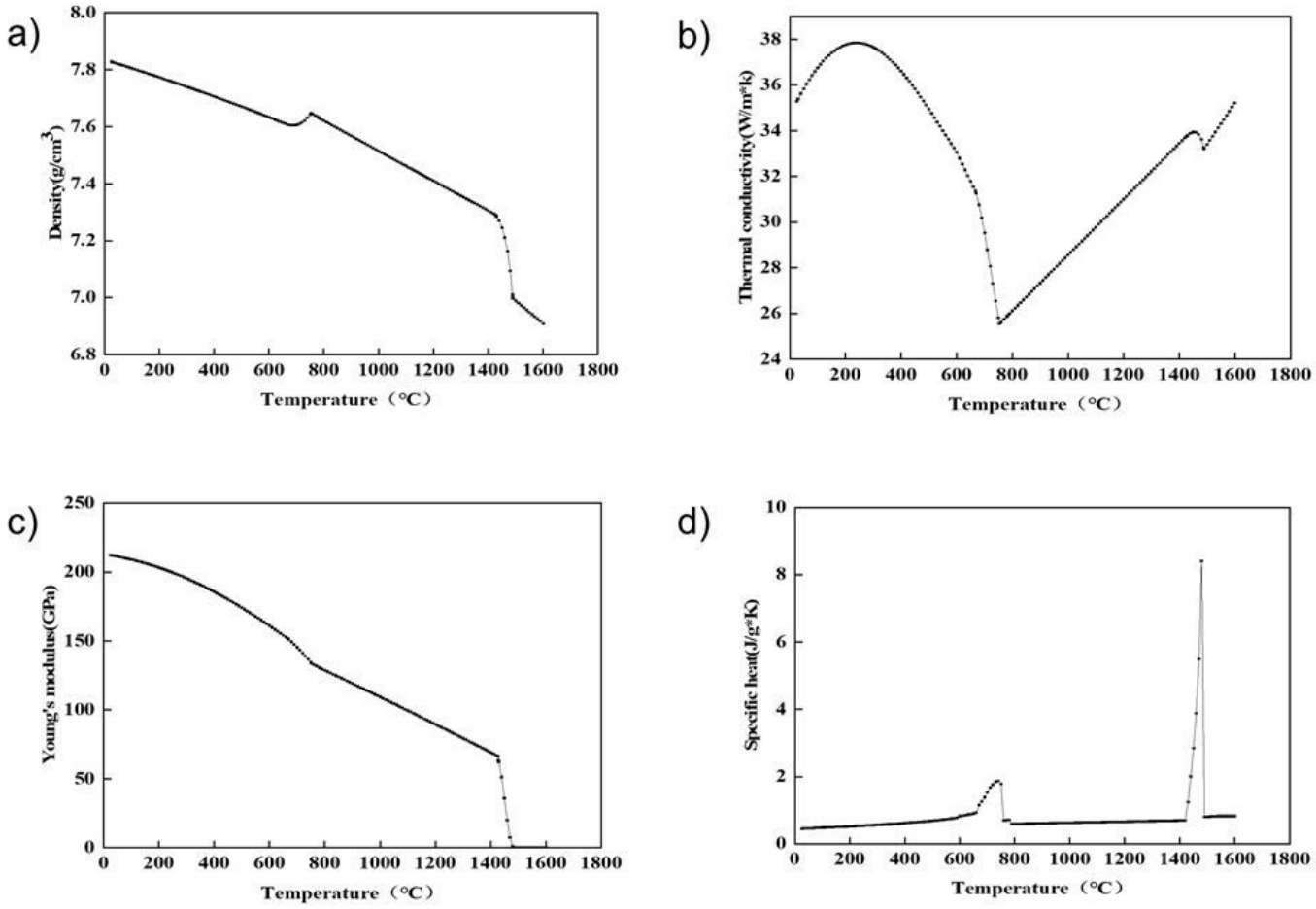

Figure 1

The thermophysical properties (a) Density, (b) Thermal conductivity, (c) Young's modulus, (d) Specific heat

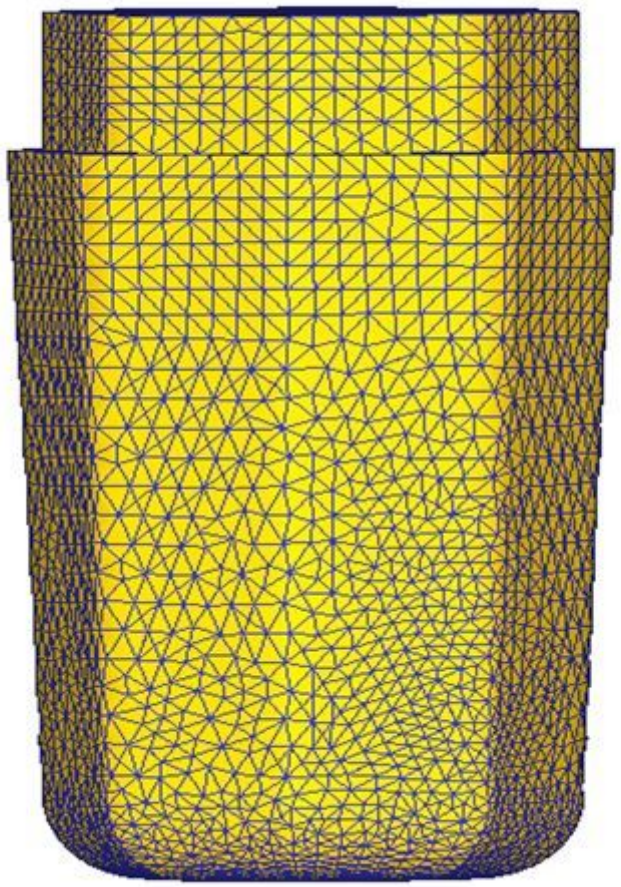

Figure 2

Finite element model

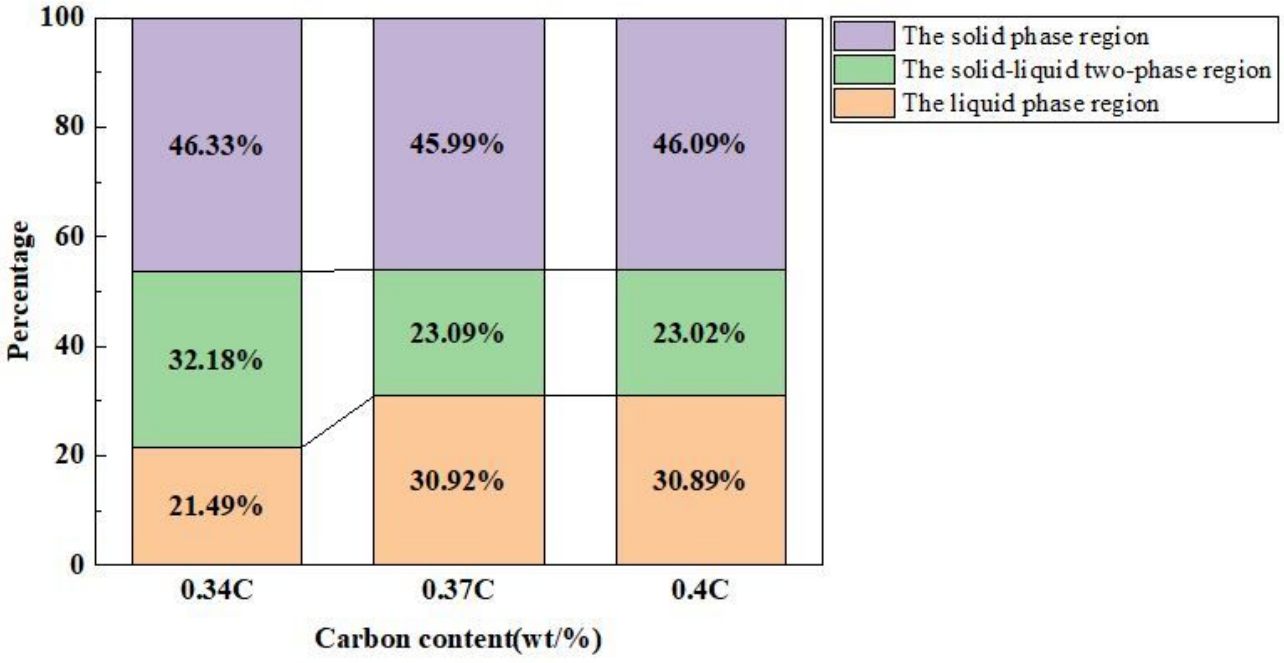

Figure 3

Percentage of each phase with 0.34%C, 0.37%C and 0.4%C after the solidification process with mold

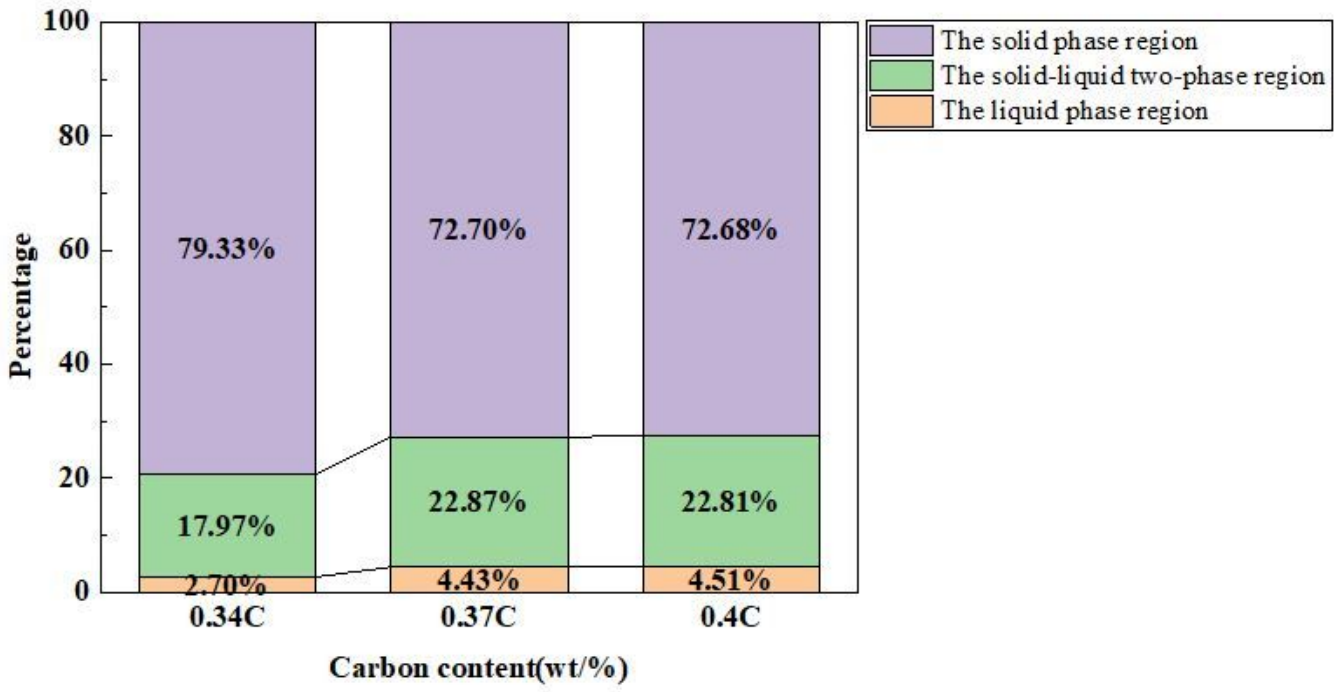

Figure 4

Percentage of each phase with 0.34%C, 0.37%C and 0.4%C after the ultra-high temperature demoulding

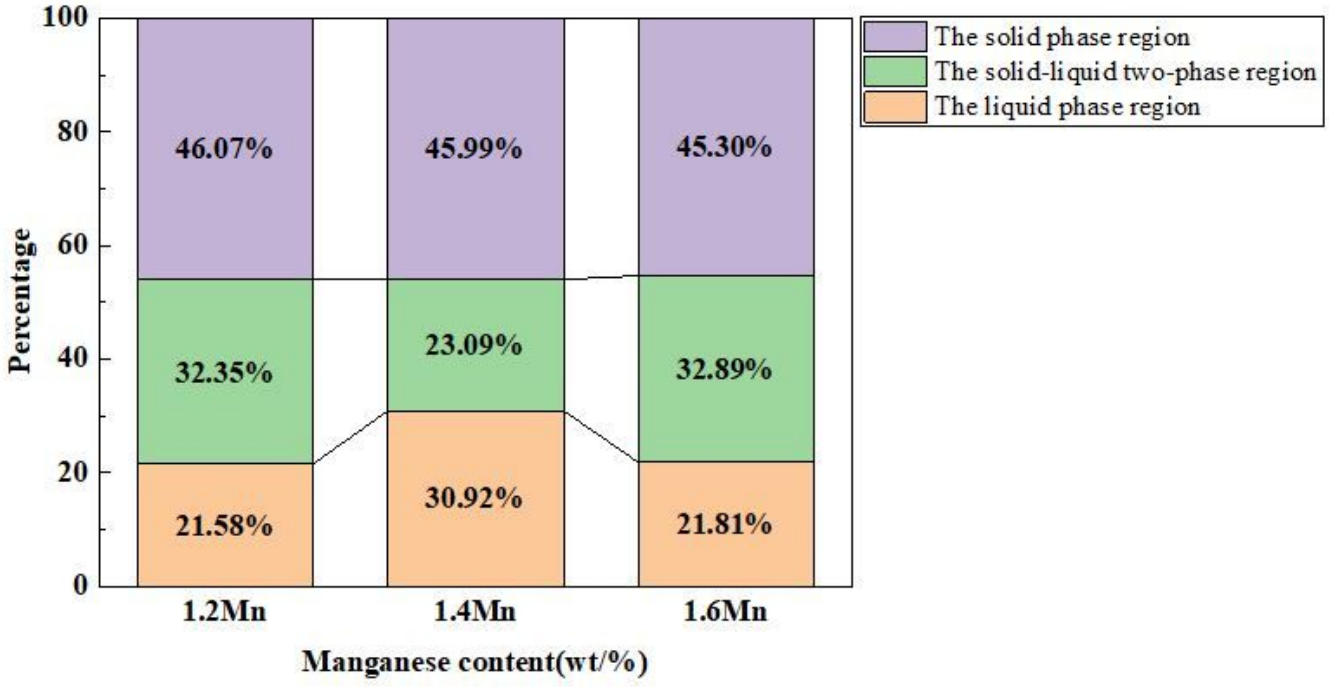

Figure 5

Percentage of each phase with 1.2%Mn, 1.4%Mn and 1.6%Mn after the solidification process with mold.

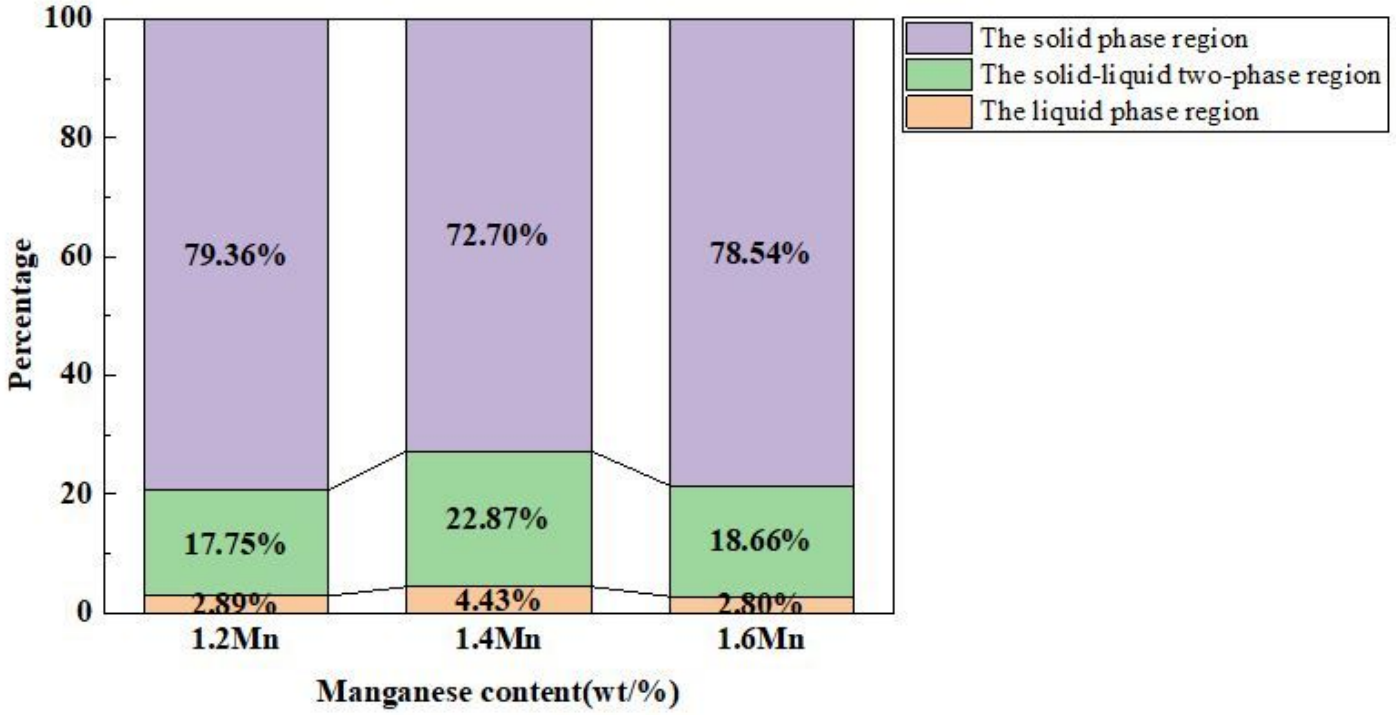

Figure 6

Percentage of each phase with 1.2%Mn, 1.4%Mn and 1.6%Mn after the ultra-high

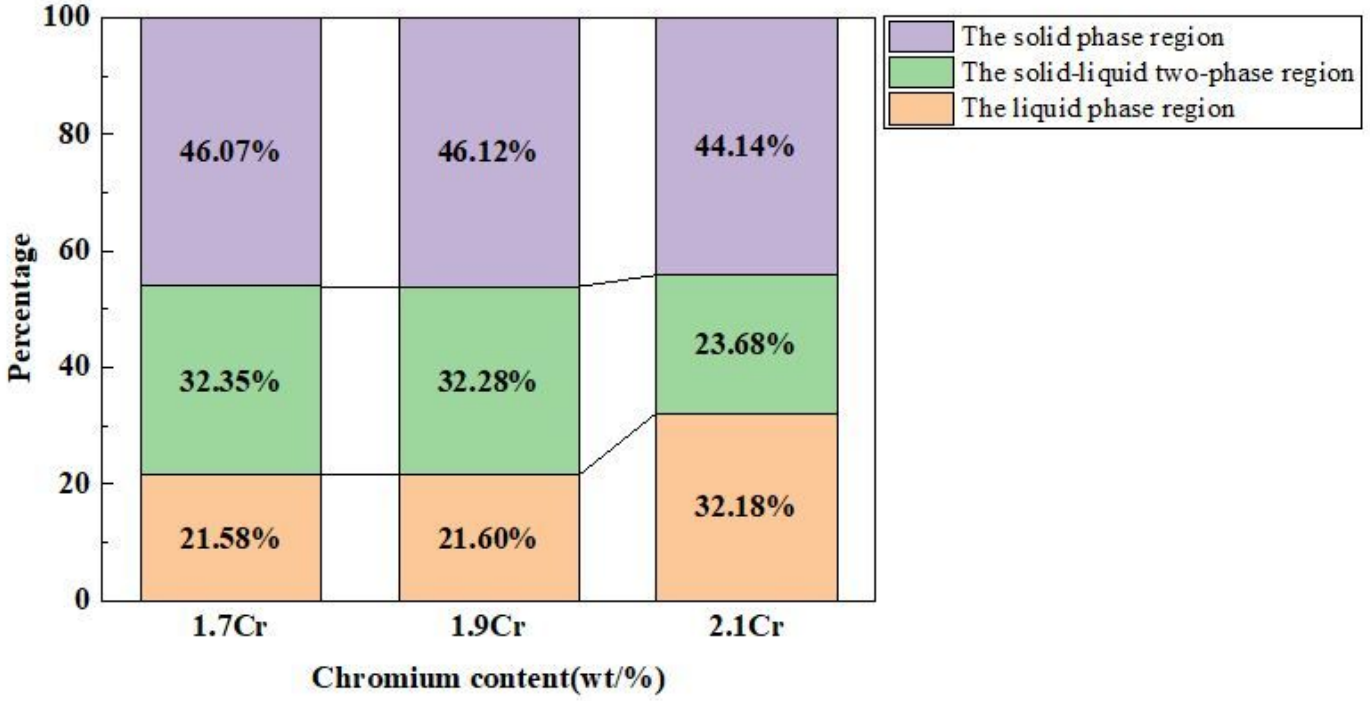

Figure 7

Percentage of each phase with 1.7%Cr, 1.9%Cr and 2.1%Cr after the solidification process with mold.

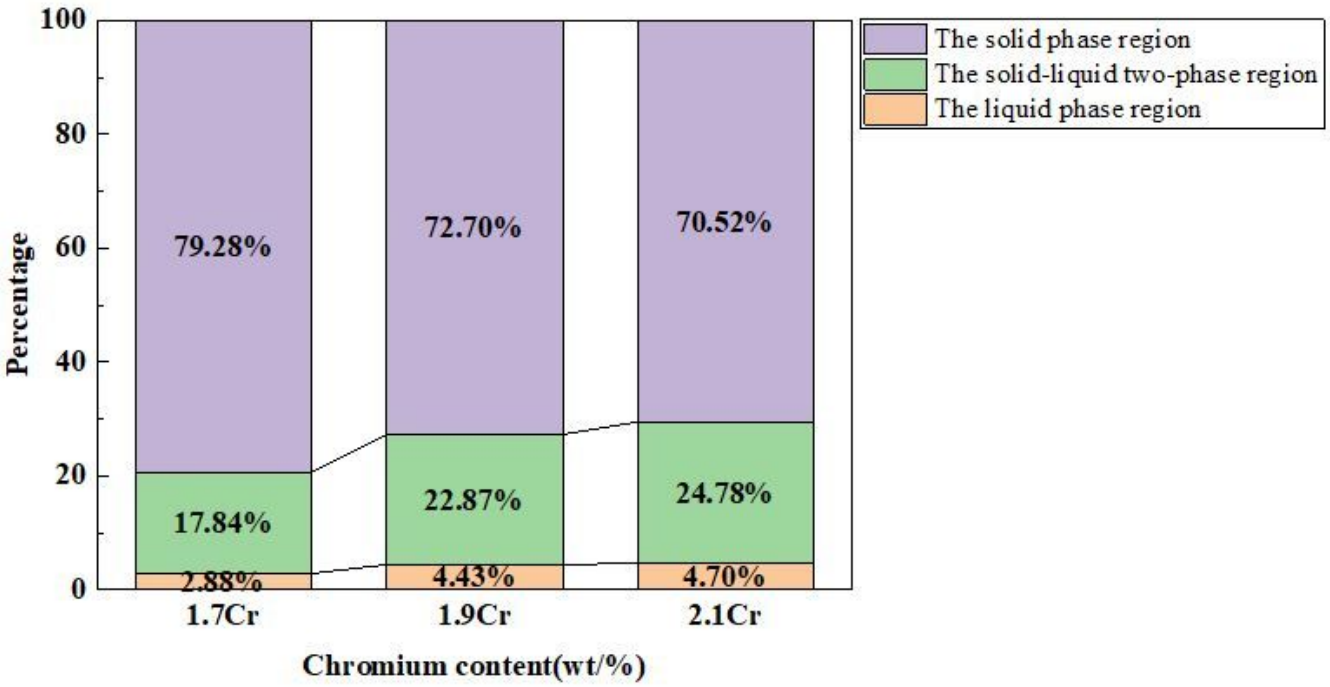

Figure 8

Percentage of each phase with 1.7%Cr, 1.9%Cr and 2.1%Cr after the ultra-high temperature demoulding

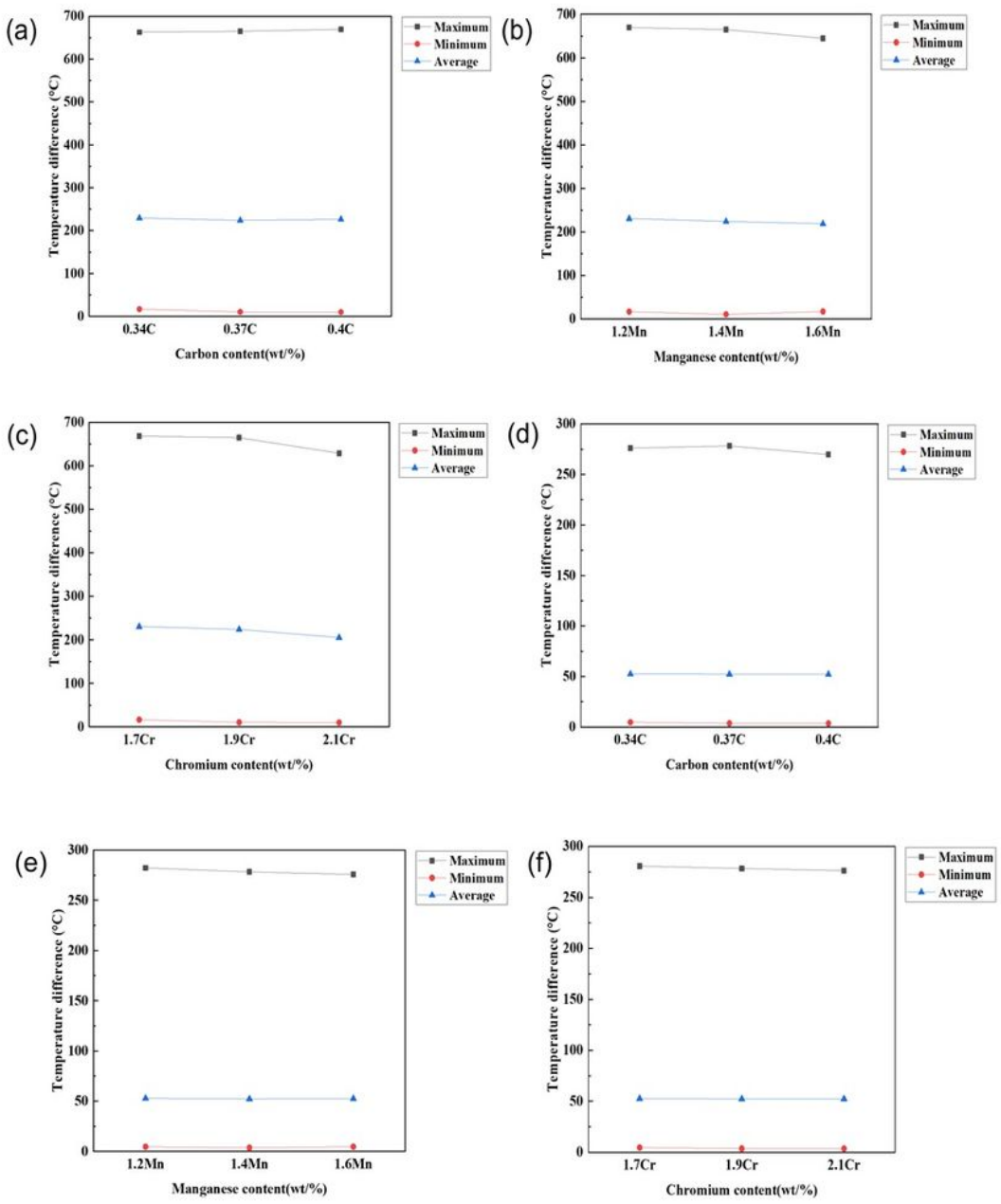

Figure 9

The temperature difference (a) the influence of C after the solidification process with mold, (b) the influence of Mn after the solidification process with mold, (c) the influence of Cr after the solidification process with mold, (d) the influence of C after the ultra-high temperature demoulding, (e) the influence of Mn after the ultra-high temperature demoulding, (f) the influence of Cr after the ultra-high temperature demoulding

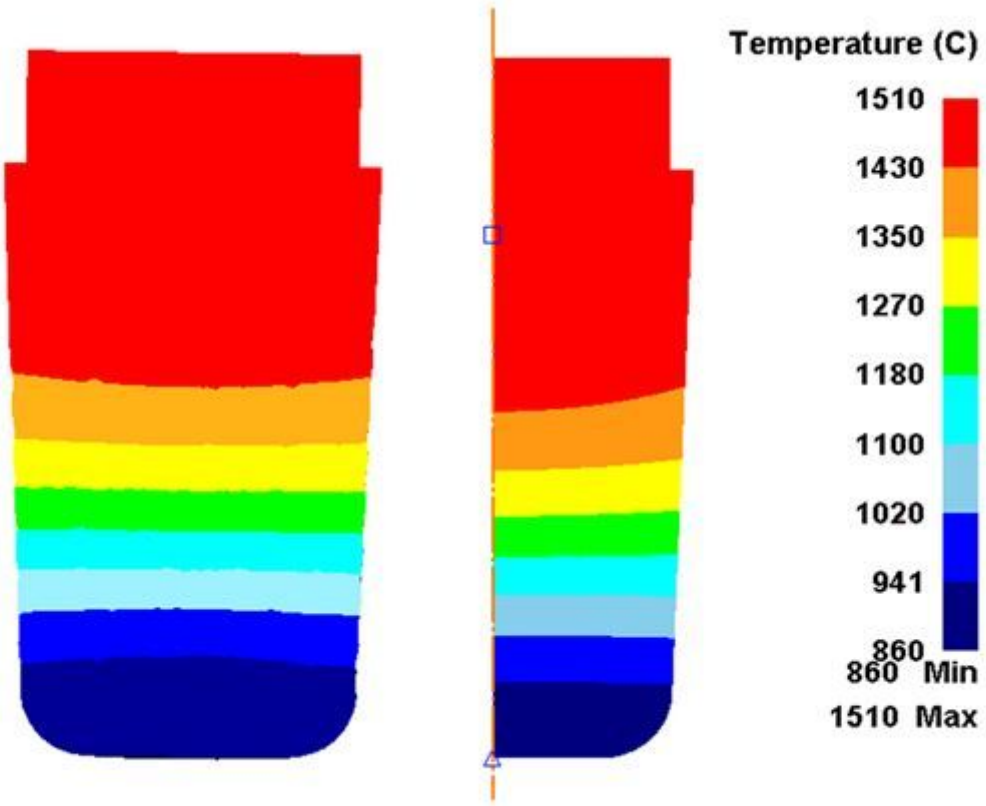

Figure 10

Comparison of temperature fields between three-dimensional models and two-dimensional ones

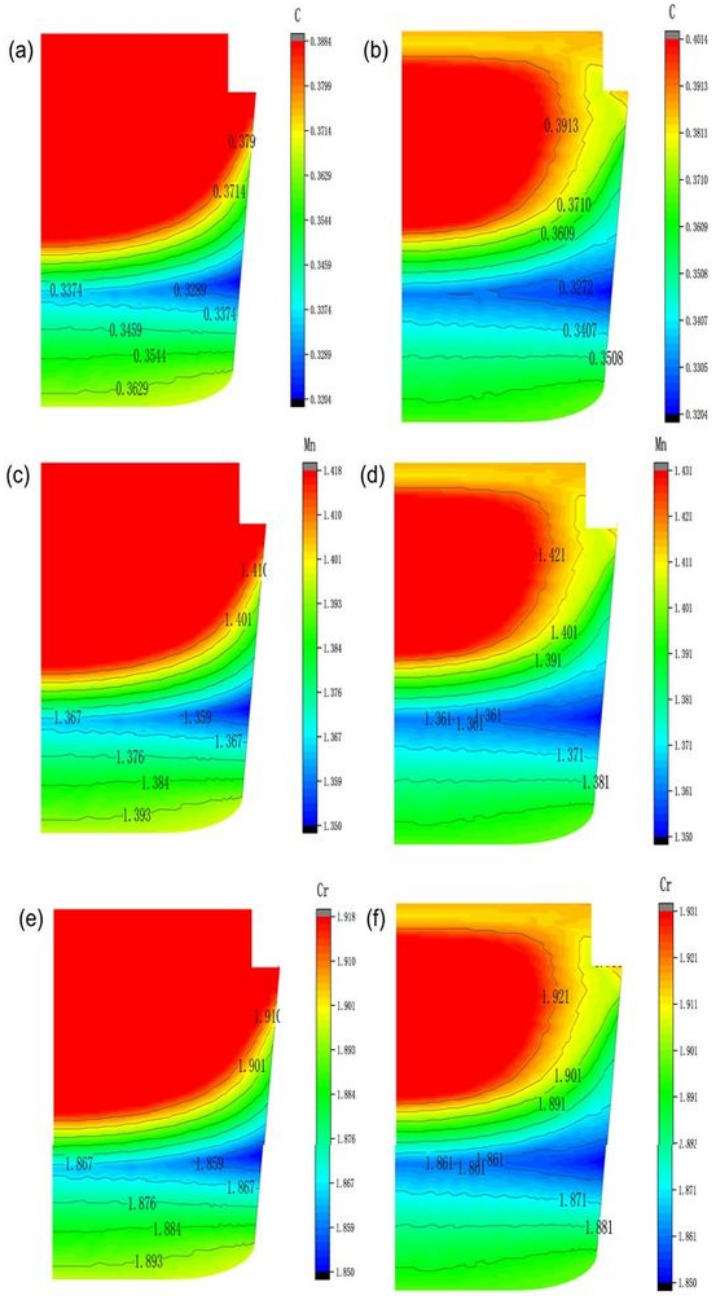

Figure 11

The concentration distribution (a) C concentrations after the solidification process with mold, (b) Mn concentrations after the solidification process with mold, (c) Cr concentrations after the solidification process with mold, (d) C concentrations after the ultra-high temperature demoulding, (e) Mn concentrations after the ultra-high temperature demoulding, (f) Cr concentrations after the ultra-high temperature demoulding.

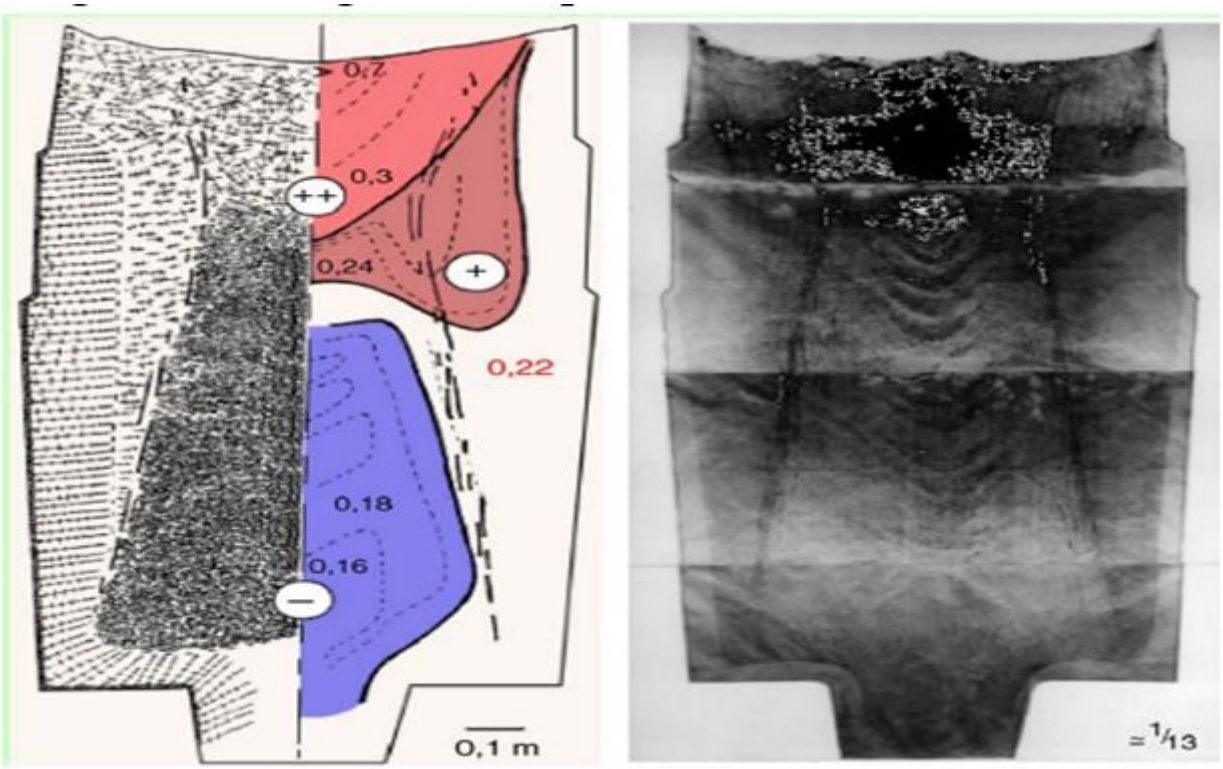

Figure 12

Lesoult's model[22]